

An Efficiency Metric for k-Space Trajectories

C. J. Hardy¹, and L. Marinelli¹

¹GE Global Research, Niskayuna, NY, United States

Introduction: When choosing among k -space trajectories to optimize imaging speed (or minimize pulse widths, for 2D excitation pulses), a two-step process is often used: first, a trajectory is selected that allows efficient traversal under conditions of constrained speed of traversal (gradient amplitude) and acceleration (slew rate). Then the rate of traversal is adjusted at each point in time to minimize the overall time required (1-6). We develop a metric (described below) for assessing the efficiency of k -space coverage for any trajectory, employing a recently described remapping algorithm (6) to continuously adjust the rate of traversal to always push gradient amplitude or slew rate to the limit over the whole course of the trajectory, yielding time-optimal gradient waveforms. Various trajectories are compared using this metric.

Methods: Five k -space trajectories (Figs. 1 and 2) were selected for comparison, each extending over a range between $\pm 1 \text{ cm}^{-1}$ in k_x and k_y , and each having similar net length ($27 \pm 2 \text{ cm}^{-1}$). Time-optimal gradient waveforms were calculated for each trajectory, using an algorithm that incorporates an arc-length formulation of the k -space traversal (6), and assuming a maximum gradient strength of 40 mT/m and a maximum slew rate of 150 mT/m/s. An example of the effect of this algorithm is given in Fig. 2, for the case of a spiral trajectory. Fig. 2a shows k -space, gradient ($= \dot{\mathbf{k}}(t) / \gamma$), and slew-rate ($= \dot{\mathbf{g}}(t)$) trajectories for the standard constant-angular-rate traversal of the spiral. After application of the algorithm, the traversal varies in such a way as to create constant slew rate over the entire pulse, resulting in the trajectories of Fig. 2b (The circular path in “slew space” is traversed 8 times here). The resulting gradient waveforms are shown in Fig. 3a, along with the RF waveform (7-8) needed to excite a 7-mm-diameter cylinder of Gaussian profile. (The resulting profile, determined by solution of the Bloch equations, is shown in Fig. 3b). Figure 4 shows two more examples of time-optimal 2D excitation pulses (left) and profiles (right), for the trajectories of Fig. 1a (top) and Fig. 1d (bottom). Note that while the spiral in the above example was limited by slew rate and not amplitude, the algorithm in general accounts for both limits, and can alternate between them over the course of the pulse.

To work well, a trajectory should have sufficient extent of k -space coverage (for resolution) and density of coverage (for field of view). The average density of coverage can be represented as the total length of the trajectory divided by the area of k -space covered. To compare trajectories, we take the range of k space to be constant ($\pm 1 \text{ cm}^{-1}$ in k_x and k_y), and define our efficiency metric ϵ to be the total length of the trajectory divided by the time of traversal (i.e. the average speed of traversal).

Results and Discussion:

Table 1 shows the time of traversal of the 5 trajectories (a-d correspond to Fig. 1 and e is the spiral) before (T_i) and after (T_o) remapping the rate of traversal, along with the efficiency ϵ of the remapped trajectory. As expected, trajectories with regions of high curvature appear to be less efficient on average than those with gentler bends. Note, the Lissajous (Fig. 1b) is different from the other 5 trajectories in that it does not lie within a circular envelope. Assuming the corners of k -space provide relatively little benefit, the relative efficiency for this trajectory can be scaled by $(\pi/4)$, yielding a final value of $\epsilon = 5.4$.

Of course, considerations other than efficiency can also be important, including off-resonance behavior, uniformity of coverage, crossing of segments, and whether the trajectory (for excitation trajectories) is Hermitian (9). These considerations will be treated as well.

References: 1) Hardy CJ, et al. J Appl Phys 1989;66:1513-1516. 2) King KF, et al. Magn Reson Med 1995;34:156-160. 3) Simonetti OP, et al. Magn Reson Med 1993;29:498-504. 4) Glover GH. Magn Reson Med 1999;42:412-415. 5) Hargreaves BA, et al. Magn Reson Med 2004;51:81-92. 6) Lustig M, et al. IEEE Trans Med Imag 2008;27:866-873. 7) Pauly J, et al. J Magn Reson 1989;81:43-56. 8) Hardy CJ, et al. J Magn Reson 1990;87:639-645. 9) Pauly J, et al. J Magn Reson 1989;82:571-587.

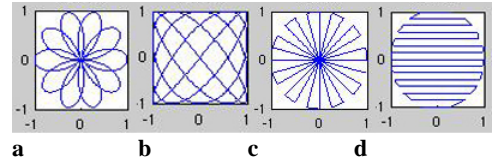


Figure 1. Four trajectories of similar length.

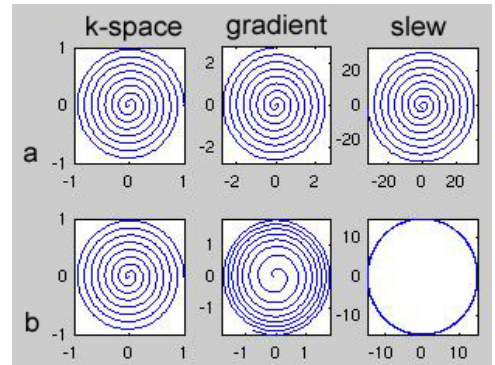


Figure 2. k -space, gradient, and slew-rate trajectories for spiral pulse with (a) constant-angular-rate k -space traversal, and (b) optimal slew-rate-limited traversal.

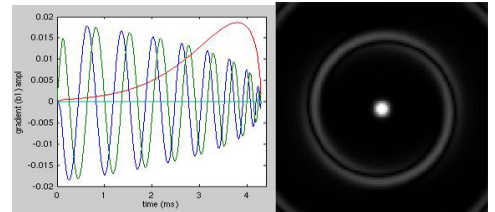


Figure 3. (a) Gradient (blue – G_x , green – G_y) and RF (red) waveforms for trajectory of Fig 2b. (b) Excitation profile for pulse.

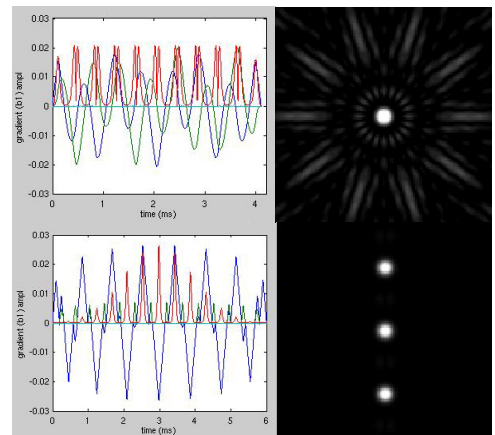


Figure 4. Optimized pulses (left) and excitation profiles (right), for trajectories of Fig. 1a (top) and Fig. 1d (bottom). G_x – blue, G_y – green, RF – red.